Int. J. Therm. Sci. (2001) 40, 877–889
© 2001 Éditions scientifiques et médicales Elsevier SAS. All rights reserved
S1290-0729(01)01274-1/FLA

Transient radiation and conduction in a two-dimensional participating cylinder subjected to a pulse irradiation

Lin-Hua Liu *, He-Ping Tan

School of Energy Science and Engineering, Harbin Institute of Technology, 92 West Dazhi Street, Harbin 150001, People's Republic of China

(Received 9 September 2000, accepted 13 December 2000)

Abstract — The transient thermal responses in a two-dimensional semitransparent cylinder with black boundary surfaces caused by a pulse irradiation at one end of the cylinder are studied. The processes of the transient coupled radiative-conductive heat transfer in the cylinder are analyzed numerically. An implicit central-difference scheme is employed for handling the energy equation, while a discrete-ordinates method is used to solve the radiative transfer equation. The effects of various parameters on the transient thermal responses are investigated. It is found that, due to the radiation within medium, the transient temperature of the nonirradiated end surface of the cylinder can be greater than that of the inner medium of cylinder. Temperature evolution curves with two peaks can be observed under some conditions at the nonirradiated end of the cylinder. The effects of the conduction-radiation parameter, the optical thickness and refractive index on the transient temperature responses are large. The effects of single-scattering albedo are more significant for the radiation-dominated case than that for the conduction-dominated case. © 2001 Éditions scientifiques et médicales Elsevier SAS

transient temperature response / coupled radiation and conduction / transient heat transfer / semitransparent medium

Nomenclature

A	area	m^{-2}
a, b	coefficients in the discretized energy equation	
c_p	specific heat	$J \cdot kg^{-1} \cdot K^{-1}$
F	time-dependent irradiation heat flux density	$W \cdot m^{-2}$
F^*	dimensionless time-dependent irradiation heat flux density	
G	incident radiation	$W \cdot m^{-3}$
G^*	dimensionless incident radiation defined in equation (21)	
g	scattering asymmetry parameter	
I	radiation intensity	$W \cdot m^{-2} \cdot sr^{-1}$
I^*	dimensionless radiation intensity defined in equation (9)	
k	thermal conductivity	$W \cdot m^{-1} \cdot K^{-1}$
L	length of cylinder	m
N	conduction-to-radiation parameter defined in equation (10)	
n	refractive index	
P	amplitude of pulse irradiation	$W \cdot m^{-2}$
P^*	dimensionless amplitude of pulse irradiation defined in equation (11)	
$\mathbf{Q}^r$	dimensionless net radiative heat flux density vector defined in equation (12)	
Q_r^r	dimensionless radial net radiative heat flux density defined in equation (13)	
Q_z^r	dimensionless axial net radiative heat flux density defined in equation (14)	
$\mathbf{q}^r$	net radiative heat flux density vector	$W \cdot m^{-2}$
q_r^r	net radial radiative heat flux density	$W \cdot m^{-2}$
q_z^r	net axial radiative heat flux density	$W \cdot m^{-2}$
R	radius	m
r	radial coordinate	m
S_C, S_P	source terms in the discretized energy equation	
S_m^*	source term in the discretized radiative transfer equation	
T	medium temperature	K
T_0	temperature of surroundings	K
t	time	s
t_{ir}	time width of pulse irradiation	s
ΔV	dimensionless volume of control-volume	
w	quadrature weight	
z	axis coordinate	m

* Correspondence and reprints.
E-mail addresses: liulh_hit@263.net (L.-H. Liu), tanhp@etp4.hit.edu.cn (H.-P. Tan).

Greek symbols

β	extinction coefficient	m^{-1}
θ	dimensionless temperature defined in equation (15)	
μ, η, ξ	direction cosines	
σ	Stefan–Boltzmann constant	$W{\cdot}m^{-2}{\cdot}K^{-4}$
τ	optical coordinate	
τ_L	axial optical thickness of cylinder	
τ_R	radial optical thickness of cylinder	
τ_r	optical coordinate in radial direction defined in equation (16)	
$\tau_{r,P}$	radial optical ordinate of nodal point	
$\tau_{r,n}$	radial optical ordinate of northern control volume surface	
$\tau_{r,s}$	radial optical ordinate of the southern control volume surface	
τ_L	axial optical thickness	
τ_z	optical coordinate in axis direction defined in equation (17)	
φ	azimuthal angle	rad
ζ	dimensionless time defined in equation (18)	
ζ_{ir}	dimensionless time width of pulse irradiation defined in equation (19)	
Φ	scattering phase function	
ω	single scattering albedo	
Ω	solid angle	sr

1. INTRODUCTION

Coupled radiative–conductive heat transfer has drawn much attention due to importance in the associated application fields such as the measurement of thermophysical properties and the thermal control by ceramics and low density refractory material. Viskanta [1] studied the steady-state radiative–conductive heat transfer problem with isotropic scattering by using the direct iterative solution to the integral form of the transfer equation. Lii and Ozisik [2] solved the transient conductive-radiative problem using Case's normal-mode expansion technique for the equation of transfer in a slab of reflecting boundaries. Amlin and Korpela [3] applied finite difference methods to solve the first order differential approximation of radiation and the energy equation for transient heat transfer in an emitting-absorbing solid. Siewert and Thomas [4–6], Siewert [7] used a computationally stable version of the spherical harmonics method and Hermite cubic splines to solve a series of one-dimensional steady-state conductive-radiative problems. Derevyanko and Koltun [8] employed the Monte Carlo method together with a finite difference method to investigate the transient interaction of radiation and conduction in the absence of scattering. Vargas and de Vilhena [9] developed a closed-form solution for the one-dimensional radiative conductive problem by the decomposition and LTS_N methods. Abulwafa [10] used the Galerkin-iterative technique to solve the couple radiative–conductive heat equations in integral forms. Tan et al. [11, 12] investigated the temperature response caused by a pulse or a step laser irradiation in semitransparent slabs with generalized boundary conditions by the ray tracing method. Andre and Degiovanni [13] studied the transient conduction-radiation heat transfer of non-scattering glass specimen. Hahn et al. [14] applied the three-flux method to calculate the temperature response caused by laser irradiation in an absorbing, isotropic scattering slab. Mehling et al. [15] developed a new analytical model to analyze the transient coupled conduction and radiation heat transfer processes in optically thin non-scattering semitransparent slabs. Spuckler and Siegel [16, 17] used the finite difference method in combination with Green's function to solve the steady-state radiative–conductive heat transfer problems in one-dimensional semitransparent slabs.

Due to the complexity of the problem, most of the work has been reported in one-dimensional geometries, only a limited amount of work is available for multidimensional cases [18–21]. Sakami et al. [18] presented a new approach for determining the radiative intensity and temperature fields in a semitransparent medium for coupled radiative–conductive heat transfer in two-dimensional complex geometrical enclosures, in which a modified discrete ordinates method based on the incorporation of directional ray propagation relations within cells was developed to handle triangular grids of any type, structured or unstructured. Li and Ozisik [19] used an finite difference method in combination with discrete ordinates method to study the steady-state coupled conduction and radiation in a two-dimensional absorbing, emitting and anisotropic scattering gray hollow and solid cylinder with gray surface. Le Dez et al. [20] employed the finite difference scheme and the ray-tracing technique to analyze a steady-state combined conductive-radiative problem in axisymmetric semitransparent bodies. Wu et al. [21] analyzed the transient two-dimensional radiative and conductive heat transfer in an axisymmetric medium heated or cooled by internal heat source or boundary, in which an finite difference scheme in combination with discrete-ordinates method was used to solve the transient coupled radiative–conductive heat transfer problem.

The objective of this work is extend the solution technique presented in ref. [19, 21] to analyze the transient thermal responses in a two-dimensional semitransparent

cylinder with black boundary surfaces caused by a pulse irradiation at one end of the cylinder. The processes of the transient coupled radiative–conductive heat transfer in the cylinder are analyzed numerically. An implicit central-difference scheme is employed for handling the energy equation, while a discrete-ordinates method is used to solve the radiative transfer equation. The effects of various parameters on the transient thermal responses will be investigated.

2. PHYSICAL MODEL AND FORMULATION

As shown in *figure 1*, we consider a gray, absorbing, emitting and scattering finite cylinder with black boundary surfaces, initially at thermal equilibrium with the surroundings. The convection with the surroundings is omitted. At time $t = 0$, a pulse is irradiated on the end surface of $z = 0$. The energy equation for transient coupled radiative and conductive heat transfer in two-dimensional semitransparent finite cylinder can be expressed as

$$\rho c_{\mathrm{p}} \frac{\partial T(z,r,t)}{\partial t} = k\left\{\frac{1}{r}\frac{\partial}{\partial r}\left(r\frac{\partial T(z,r,t)}{\partial r}\right) + \frac{\partial^2 T(z,r,t)}{\partial z^2}\right\} - \nabla\cdot\mathbf{q}^{\mathrm{r}}(z,r,t) \tag{1a}$$

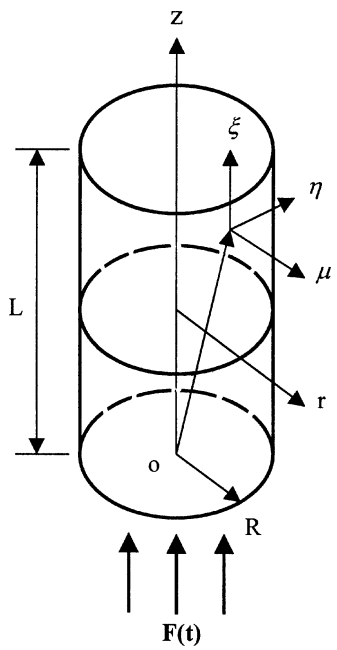

Figure 1. Schematic of the physical system and coordinates.

where ρ is the density of medium, c_{p} is the specific heat, T is the temperature, k is the thermal conductivity, $\mathbf{q}^{\mathrm{r}}$ is the net radiative heat flux density vector, z, r and t are the space and time coordinates, respectively.

The boundary, symmetry and initial conditions are given as:

$$\partial T(z,r,t)/\partial r = 0, \quad r = 0 \tag{1b}$$

$$-k\partial T(z,r,t)/\partial r = \sigma\left[T^4(z,R,t) - T_0^4\right] - q_r^{\mathrm{r}}(z,R,t), \quad r = R \tag{1c}$$

$$-k\partial T(z,r,t)/\partial z = F(t) - \sigma\left[T^4(0,r,t) - T_0^4\right] - q_z^{\mathrm{r}}(0,r,t), \quad z = 0 \tag{1d}$$

$$-k\partial T(z,r,t)/\partial z = \sigma\left[T^4(L,r,t) - T_0^4\right] - q_z^{\mathrm{r}}(L,r,t), \quad z = L \tag{1e}$$

$$T(z,r,0) = T_0, \quad t = 0 \tag{1f}$$

where T_0 is the temperature of the surroundings, $F(t)$ is the time-dependent irradiation heat flux density, σ is the Stefan–Boltzmann constant, q_r^{r} and q_z^{r} are the radial and axial net radiative heat flux densities, respectively.

In this paper, we consider a step pulse irradiation represented mathematically in the form

$$F(t) = \begin{cases} P, & 0 \leqslant t \leqslant t_{\mathrm{ir}} \\ 0, & t > t_{\mathrm{ir}} \end{cases} \tag{2}$$

where P is the amplitude of pulse irradiation, t_{ir} is the time width of the pulse irradiation.

The radiative transfer equation in a two-dimensional semitransparent finite cylinder with black boundary surfaces can be written as [22]

$$\frac{\mu}{r}\frac{\partial[rI(z,r,\mu,\eta,\xi,t)]}{\partial r} - \frac{1}{r}\frac{\partial[\eta I(z,r,\mu,\eta,\xi,t)]}{\partial\varphi} + \xi\frac{\partial I(z,r,\mu,\eta,\xi,t)}{\partial z} = -\beta I(z,r,\mu,\eta,\xi,t) + \beta(1-\omega)I_{\mathrm{b}}(T) + \frac{\beta\omega}{4\pi}\int_{\Omega'=4\pi} I(z,r,\mu,\eta,\xi,t)\Phi\left(\Omega',\Omega\right)\mathrm{d}\Omega' \tag{3a}$$

with boundary and symmetry conditions:

$$I(z,0,\mu,\eta,\xi,t) = I(z,0,-\mu,\eta,\xi,t), \quad \mu > 0,\ r = 0 \tag{3b}$$

$$I(z, R, \mu, \eta, \xi, t) = \frac{n^2 \sigma T^4(z, R, t)}{\pi}$$
$$\mu < 0,\ r = R \tag{3c}$$
$$I(0, r, \mu, \eta, \xi, t) = \frac{n^2 \sigma T^4(0, r, t)}{\pi}$$
$$\xi > 0,\ z = 0 \tag{3d}$$
$$I(L, r, \mu, \eta, \xi, t) = \frac{n^2 \sigma T^4(L, r, t)}{\pi}$$
$$\xi < 0,\ z = L \tag{3e}$$

where I is the radiation intensity, ω is the single-scattering albedo, φ is the azimuthal angle, I_b is the blackbody radiation intensity, $\Phi(\Omega', \Omega)$ is the phase function from the incoming direction Ω' to the outgoing direction Ω, n is the refractive index, μ, η, and ξ are the direction cosines, β is the extinction coefficient.

The divergence of net radiative heat flux density vector is defined as

$$\nabla \cdot \mathbf{q}^\mathrm{r} = (1-\omega)\beta\left(4n^2\sigma T^4 - G\right) \tag{4}$$

where the incident radiation is related to radiation intensity by

$$G = \int_{\Omega=4\pi} I \,\mathrm{d}\Omega \tag{5}$$

For convenience of analysis, equations (1)–(3) are nondimensionalized, we have

$$\frac{\partial\theta}{\partial\zeta} = \frac{1}{\tau_r}\frac{\partial}{\partial\tau_r}\left(\tau_r\frac{\partial\theta}{\partial\tau_r}\right) + \frac{\partial^2\theta}{\partial\tau_z^2} - \frac{1}{N}\nabla^*\cdot\mathbf{Q}^\mathrm{r} \tag{6a}$$
$$\partial\theta/\partial\tau_r = 0, \quad \tau_r = 0 \tag{6b}$$
$$-\frac{\partial\theta}{\partial\tau_r} = \frac{1}{N}\left[\frac{\theta^4-1}{4n^2} - Q_r^\mathrm{r}\right], \quad \tau_r = \tau_\mathrm{R} \tag{6c}$$
$$-\frac{\partial\theta}{\partial\tau_z} = \frac{1}{N}\left[F^*(\zeta) - \frac{\theta^4-1}{4n^2} - Q_z^\mathrm{r}\right], \quad \tau_z = 0 \tag{6d}$$
$$-\frac{\partial\theta}{\partial\tau_z} = \frac{1}{N}\left[\frac{\theta^4-1}{4n^2} - Q_z^\mathrm{r}\right], \quad \tau_z = \tau_\mathrm{L} \tag{6e}$$
$$\theta = 1, \qquad \zeta = 0 \tag{6f}$$

$$F^*(\zeta) = \begin{cases} P^*, & 0 \leqslant \zeta \leqslant \zeta_\mathrm{ir} \\ 0, & \zeta > \zeta_\mathrm{ir} \end{cases} \tag{7}$$

$$\frac{\mu}{\tau_r}\frac{\partial(\tau_r I^*)}{\partial\tau_r} - \frac{1}{\tau_r}\frac{\partial(\eta I^*)}{\partial\varphi} + \xi\frac{\partial I^*}{\partial\tau_z} + I^* = (1-\omega)\theta^4 + \frac{\omega}{4\pi}\int_{\Omega'=4\pi} I^*(\Omega')\Phi(\Omega', \Omega)\,\mathrm{d}\Omega' \tag{8a}$$

$$I^*(\mu, \eta, \xi) = I^*(-\mu, \eta, \xi), \quad \mu > 0,\ \tau_r = 0 \tag{8b}$$
$$I^* = \theta^4, \quad \mu < 0,\ \tau_r = \tau_\mathrm{R} \tag{8c}$$
$$I^* = \theta^4, \quad \xi > 0,\ \tau_z = 0 \tag{8d}$$
$$I^* = \theta^4, \quad \xi < 0,\ \tau_z = \tau_\mathrm{L} \tag{8e}$$

Here, the dimensionless radiation intensity I^*, the conduction-to-radiation parameter N, the dimensionless amplitude of pulse irradiation P^*, the dimensionless net radiative heat flux density vector $\mathbf{Q}^\mathrm{r}$, the dimensionless radial net radiative heat flux density Q_r^r, the dimensionless axial net radiative heat flux density Q_z^r, the dimensionless temperature θ, the optical thickness variables τ_r and τ_z, the dimensionless time coordinate ζ and the dimensionless time width of the pulse irradiation ζ_ir are defined respectively as following:

$$I^* = \frac{\pi I}{\sigma T_0^4} \tag{9}$$
$$N = \frac{k\beta}{4n^2\sigma T_0^4} \tag{10}$$
$$P^* = \frac{P}{4n^2\sigma T_0^4} \tag{11}$$
$$\mathbf{Q}^\mathrm{r} = \frac{\mathbf{q}^\mathrm{r}}{4n^2\sigma T_0^4} \tag{12}$$
$$Q_r^\mathrm{r} = \frac{q_r^\mathrm{r}}{4n^2\sigma T_0^4} \tag{13}$$
$$Q_z^\mathrm{r} = \frac{q_z^\mathrm{r}}{4n^2\sigma T_0^4} \tag{14}$$
$$\theta = \frac{T}{T_0} \tag{15}$$
$$\tau_r = r\beta \tag{16}$$
$$\tau_z = z\beta \tag{17}$$
$$\zeta = \frac{k}{\rho c_\mathrm{p}}\beta^2 t \tag{18}$$
$$\zeta_\mathrm{ir} = \frac{k}{\rho c_\mathrm{p}}\beta^2 t_\mathrm{ir} \tag{19}$$

The divergence of the dimensionless net radiation heat flux density vector $\nabla^*\cdot\mathbf{Q}^\mathrm{r}$ in equation (6a) can be expressed as

$$\nabla^*\cdot\mathbf{Q}^\mathrm{r} = (1-\omega)\left(\theta^4 - G^*\right) \tag{20}$$

and the dimensionless incident radiation is defined as

$$G^* = \frac{1}{4n^2\pi}\int_{\Omega=4\pi} I^*\,\mathrm{d}\Omega \tag{21}$$

3. METHOD OF SOLUTION

Equations (6)–(8) provide the complete mathematical formulation for the transient coupled radiation and conduction in a two-dimensional semitransparent finite cylinder. An iterative process is needed to solve the problem, because the energy equation and its boundary conditions involve the dimensionless incident radiation G^*, while the radiative transfer equation requires the temperature distribution θ.

The calculated domain in $\tau_r - \tau_z$ plane was divided into uniform control volume elements by Patankar's B method [23], and a unit polar angle was used. Using an implicit central-difference approximation, a control volume form of the energy equation can be obtained by considering the integration of equation (6a) over a mesh cell with a in axisymmetric cylindrical geometry. The discretized energy equation can be written in the form [23]

$$a_{\mathrm{P}}\theta_{\mathrm{P}} = a_{\mathrm{E}}\theta_{\mathrm{E}} + a_{\mathrm{W}}\theta_{\mathrm{W}} + a_{\mathrm{N}}\theta_{\mathrm{N}} + a_{\mathrm{S}}\theta_{\mathrm{S}} + b \tag{22a}$$

where the dimensionless temperatures with subscripts E, W, etc., denote the eastern, western, etc., nodal dimensionless temperature, and

$$a_{\mathrm{E}} = a_{\mathrm{W}} = \frac{\tau_{r,\mathrm{P}}\Delta\tau_r}{\Delta\tau_z} \tag{22b}$$

$$a_{\mathrm{N}} = \frac{\tau_{r,n}\Delta\tau_z}{\Delta\tau_r} \tag{22c}$$

$$a_{\mathrm{S}} = \frac{\tau_{r,s}\Delta\tau_z}{\Delta\tau_r} \tag{22d}$$

$$a_{\mathrm{P}}^0 = \frac{\Delta V}{\Delta\zeta} \tag{22e}$$

$$S_{\mathrm{P}} = -\frac{(1-\omega)}{N}\left[\theta_{\mathrm{P}}^0\right]^3 \tag{22f}$$

$$S_{\mathrm{C}} = \frac{(1-\omega)}{N}G^* \tag{22g}$$

$$\Delta V = \tau_{r,\mathrm{P}}\Delta\tau_r\Delta\tau_z \tag{22h}$$

$$b = S_{\mathrm{C}}\Delta V + a_{\mathrm{P}}^0\theta_{\mathrm{P}}^0 \tag{22i}$$

$$a_{\mathrm{P}} = a_{\mathrm{E}} + a_{\mathrm{W}} + a_{\mathrm{N}} + a_{\mathrm{S}} + a_{\mathrm{P}}^0 - S_{\mathrm{P}}\Delta V \tag{22j}$$

Here, the variables with subscripts n, s, etc., indicate that the values have to be taken at the northern, southern, etc., control volume surfaces, respectively. θ_{P}^0 is the dimensionless nodal temperature at the old time level, $\Delta\tau_r$ is the radial optical thickness of control volume, $\Delta\tau_z$ is the axial optical thickness of control volume, $\tau_{r,\mathrm{P}}$ is the radial optical ordinate of the nodal point P, $\tau_{r,s}$ is the radial optical ordinate of the southern control volume surface, $\tau_{r,n}$ is the radial optical ordinate of northern control volume surface, and ΔV is the dimensionless volume of a control-volume. The boundary conditions of the energy equation are handled by the method of additional source term, and the discretized energy equation (22a) is solved by the ADI line iteration method.

Equations (8a)–(8e) for radiative transfer are solved by the discrete ordinates method. The S_6 solution can yield sufficiently accurate results with reasonable computer time [18, 24], therefore, in this paper, the S_6 approximation is used to solve the radiative transfer equation. In this approach, the solid angle is discretized into a finite number of directions. The equation of radiative transfer is evaluated at each of the discrete directions, and the integral of in-scattering term is replaced by a weighted sum, which leads to the discrete ordinates equations

$$\frac{\mu_m}{\tau_r}\frac{\partial(\tau_r I_m^*)}{\partial\tau_r} - \frac{1}{\tau_r}\frac{\partial(\eta_m I_m^*)}{\partial\varphi} + \xi_m\frac{\partial I_m^*}{\partial\tau_z} + I_m^* = (1-\omega)\theta^4 + \frac{\omega}{4\pi}\sum_{m'} w_{m'}\Phi_{m'm}I_{m'}^* \tag{23}$$

where subscripts m and m' represent the discrete directions, w_m are correspondingly the quadrature weights. A control volume form of the discrete-ordinates equations can be obtained by integrating equation (23) over the cell volume, from which we have [25]

$$\mu_m\left(A_n I_{m,n}^* - A_s I_{m,s}^*\right) - (A_n - A_s)\frac{\alpha_{m+1/2}I_{m+1/2}^* - \alpha_{m-1/2}I_{m-1/2}^*}{w_m} + \xi_m\left(A_{\mathrm{e}}I_{m,\mathrm{e}}^* - A_{\mathrm{w}}I_{m,\mathrm{w}}^*\right) + I_{m,\mathrm{P}}^*\Delta V = S_m^*\Delta V \tag{24a}$$

where

$$S_m^* = (1-\omega)\theta_{\mathrm{P}}^4 + \frac{\omega}{4\pi}\sum_{m'=1}^{M} w_{m'}\Phi_{m'm}I_{m'}^* \tag{24b}$$

$$A_n = \tau_{r,n}\Delta\tau_z \tag{24c}$$

$$A_s = \tau_{r,s}\Delta\tau_z \tag{24d}$$

$$A_{\mathrm{e}} = A_{\mathrm{w}} = \tau_{r,\mathrm{P}}\Delta\tau_r \tag{24e}$$

In equation (24a), the coefficients, $\alpha_{m+1/2}$ and $\alpha_{m-1/2}$, result from azimuthal difference term. The α terms are chosen to preserve the conservation of energy, i.e., the intergration of the term $\partial(\eta_m I_m^*)/\partial\varphi$ over all 2π azimutal angle must be equal to zero. The detail about the selection of $\alpha_{m+1/2}$, $\alpha_{m-1/2}$, μ_m, ξ_m and ω_m can be seen in ref. [19], and will not be repeated here. To close the above

system of equations, relations are needed between the dimensionless radiative intensities on the control volume surfaces and the nodal dimensionless radiative intensities. In this study, the diamond difference scheme is used as following

$$I^*_{m,n} + I^*_{m,s} = I^*_{m,\mathrm{e}} + I^*_{m,\mathrm{w}} = I^*_{m-1/2} + I^*_{m+1/2} = 2I^*_{m,\mathrm{P}} \tag{25}$$

The intensity at the center of control volume element can therefore be evaluated as

$$\begin{aligned} I^*_m = \Bigg(& \mu_m (A_n + A_s) I^*_{m,s} \\ & - \frac{(\alpha_{m-1/2} + \alpha_{m+1/2})(A_n - A_s)}{w_m} I^*_{m-1/2} \\ & + \xi_m (A_\mathrm{e} + A_\mathrm{w}) I^*_{m,\mathrm{w}} + S^*_m \Delta V \Bigg) \\ & \times \Bigg(2\mu_m A_n - \frac{2\alpha_{m+1/2}(A_n - A_s)}{w_m} \\ & + 2\xi_m A_\mathrm{e} + \Delta V \Bigg)^{-1} \end{aligned} \tag{26}$$

Equation (26) is applied to the case $\mu_m > 0$, $\xi_m > 0$ when the calculation proceeds in the direction of increasing τ_r and τ_z. For other combinations of μ_m and ξ_m, similar equations can be obtained.

The solution to the discrete-ordinates equations of radiative transfer must be obtained iteratively. Once the intensity at a cell center is known from equation (26), the downstream surface of volume element can be obtained by extrapolation using equation (25). The detailed procedure of solution can be seen in ref. [19, 25], and will not be repeated here. Once the dimensionless radiation intensity is known, the dimensionless incident radiation and net radiation flux density are determined approximately from their definitions as

$$G^* = \frac{1}{4n^2\pi} \sum_{m=1}^{M} w_m I^*_m \tag{27}$$

$$Q^{\mathrm{r}}_r = \frac{1}{4n^2\pi} \sum_{m=1}^{M} w_m \mu_m I^*_m \tag{28}$$

$$Q^{\mathrm{r}}_z = \frac{1}{4n^2\pi} \sum_{m=1}^{M} w_m \xi_m I^*_m \tag{29}$$

Because the energy equation contains a radiation source term, the conduction equation and the radiative heat transfer equation need to be solved iteratively. The iteration procedure at the kth time level is given as following:

Step 1: Set $\theta^{\mathrm{old}} = \theta_{k-1}$. Here, θ_{k-1} is the dimensionless temperature distribution of the $(k-1)$th time level.

Step 2: Based on the dimensionless temperature distribution θ^{old}, solve the radiative transfer equation, and calculate the dimensionless net radiative heat flux density.

Step 3: Knowing the dimensionless net radiative heat flux density, solve the energy equation, and calculate the dimensionless temperature distribution θ^{new}.

Step 4: Terminate the iteration process of the kth time level and go to the next time level if the following specified stopping criterion is satisfied at each grid point,

$$\left|\theta^{\mathrm{old}} - \theta^{\mathrm{new}}\right| / \theta^{\mathrm{old}} < 10^{-4} \tag{30}$$

Otherwise, go to step 5.

Step 5: Set $\theta^{\mathrm{old}} = \theta^{\mathrm{new}}$, and go back to step 2.

4. RESULTS AND DISCUSSION

A computer code was written based on the above calculation procedure. Grid refinement and time step sensitivity studies were also performed for the physical model to ensure that the essential physics are independent of grid size and time interval. In the following analysis, the scattering phase function of media is assumed to be linear anisotropic, given as

$$\Phi(\Omega', \Omega) = 1 + g(\mu'\mu + \eta'\eta + \xi'\xi) \tag{31}$$

where g is the scattering asymmetry parameter.

Figure 2 shows the transient temperature responses at the dimensionless time $\zeta = 0.01$ and $\zeta = 0.03$ in the case of $N = 7$, $n = 1$, $\tau_\mathrm{L} = 0.4$, $\tau_\mathrm{R} = 0.1$, $\omega = 0.5$, $g = 0.5$, $\zeta_{\mathrm{ir}} = 0.01$ and $P^* = 1000$. As shown in *figure 2*, it can be seen that, due to the radiation within medium, the transient temperature of the nonirradiated end surface ($\tau_z = \tau_\mathrm{L}$) of the cylinder can be greater than that of the inner medium of cylinder. After irradiation turn-off, due to the radiation cooling of surrounding, the temperature of cylinder decreases gradually and the temperature of inner medium will be greater than that of boundary surface.

The conduction-to-radiation parameter N characterizes the relative importance of conduction in regard to radiation. *Figures 3* and *4* show the influences of conduction-to-radiation parameter on the transient tem-

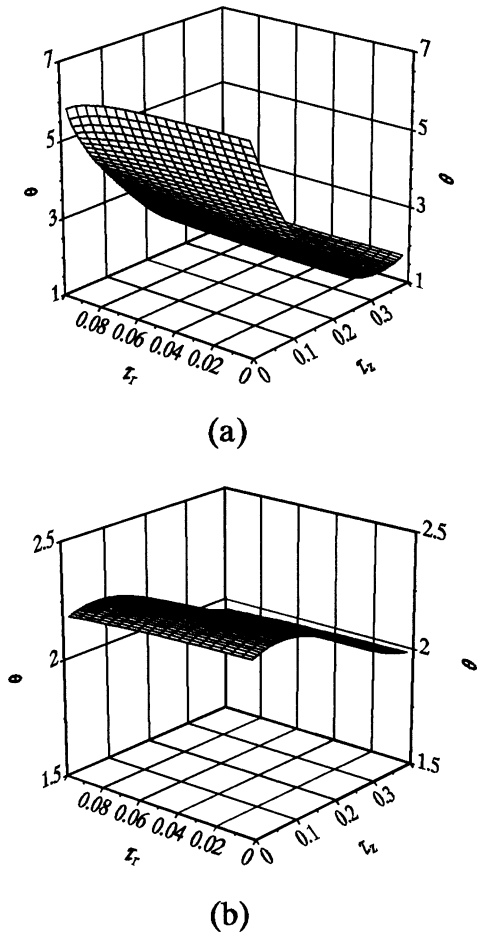

Figure 2. The transient temperature responses in the case of $N = 7$, $n = 1$, $\tau_L = 0.4$, $\tau_R = 0.1$, $\omega = 0.5$, $g = 0.5$, $\zeta_{ir} = 0.01$ and $P^* = 1000$: (a) $\zeta = 0.01$; (b) $\zeta = 0.03$.

perature responses in the case of $n = 1$, $\tau_L = 0.4$, $\tau_R = 0.1$, $\omega = 0.5$, $g = 0.5$, $\zeta_{ir} = 0.01$ and $P^* = 1000$. As shown in *figures 3* and *4*, the effects of conduction-to-radiation parameter on the transient temperature responses are significant. Because of the radiation interaction within medium, the temperature rising velocity at the nonirradiated end surface decreases with the increase of N (*figure 3*), and the spatial temperature distribution within the cylinder becomes more even when N decreases (*figure 4*). It is also found that, in some conditions, due to the competition between radiation and conduction, for example, $N = 7$ and $N = 10$ in *figure 3*, the temperature evolution curves with two peaks can be observed at the nonirradiated end of the cylinder. The first peak results from the direct radiative heating of the hot irradiated face. In the case of *figure 3*, the axial optical thickness τ_L of the cylinder is equal to 0.4, a part about

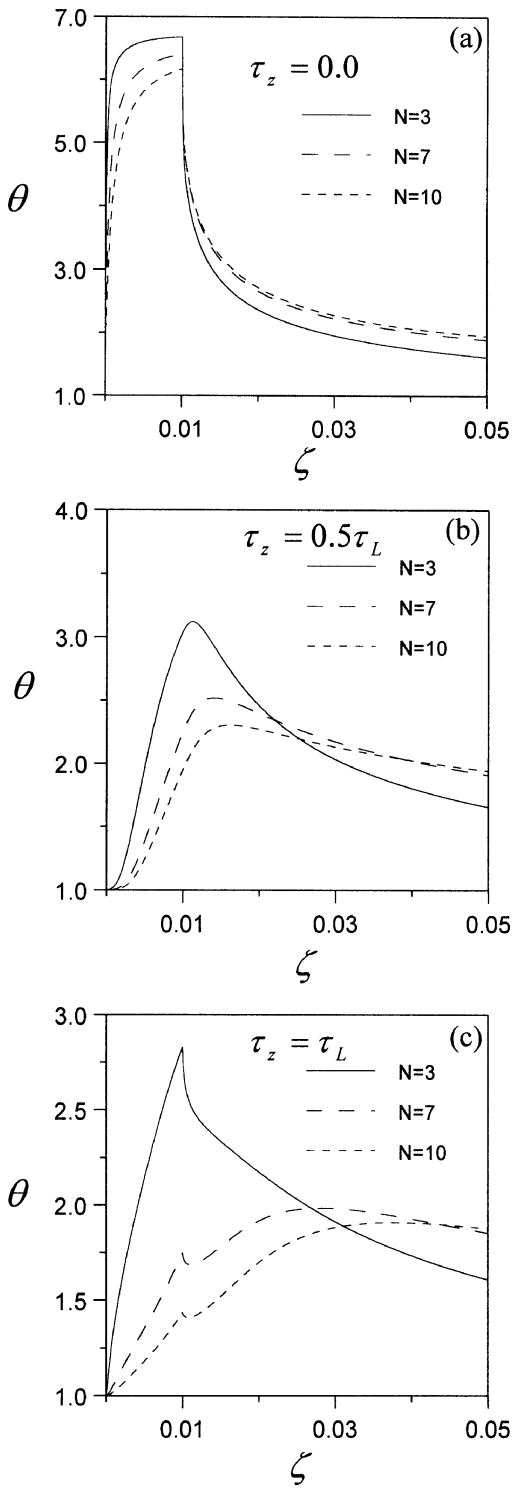

Figure 3. The effects of conduction-to-radiation parameter on the transient temperature responses at the surfaces of $\tau_z = 0$, $\tau_z = 0.5\tau_L$ and $\tau_z = \tau_L$, for the case of $n = 1$, $\tau_L = 0.4$, $\tau_R = 0.1$, $\omega = 0.5$, $g = 0.5$, $\zeta_{ir} = 0.01$ and $P^* = 1000$.

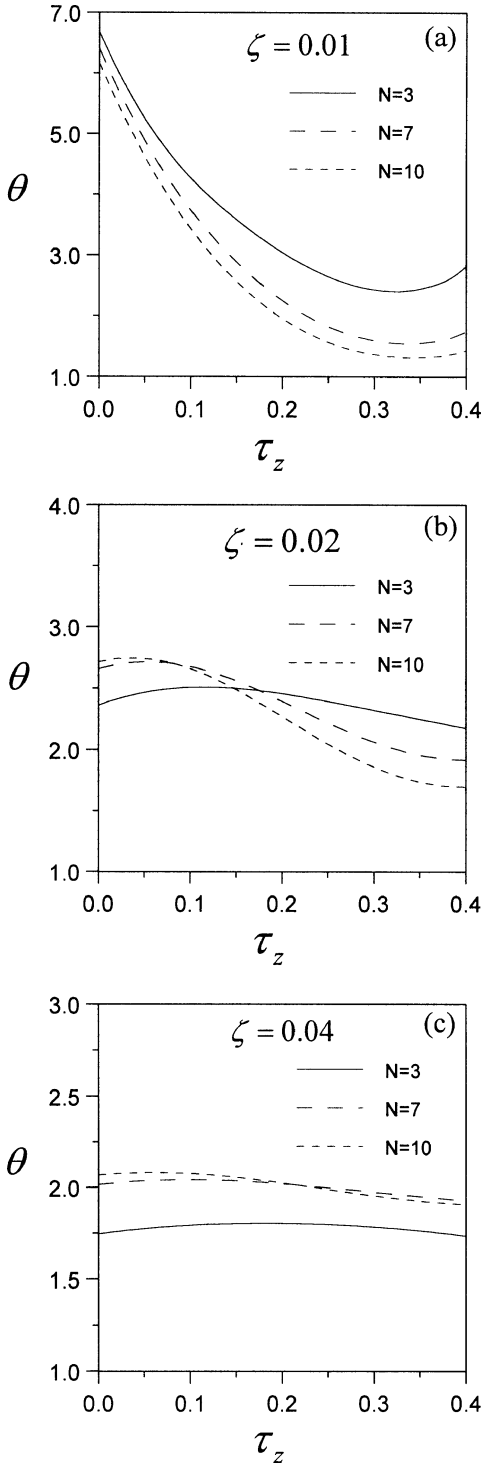

Figure 4. The effects of conduction-to-radiation parameter on the axial temperature distribution of cylinder centerline at the dimensionless time $\zeta = 0.01$, $\zeta = 0.02$ and $\zeta = 0.03$ for the case of $n = 1$, $\tau_L = 0.4$, $\tau_R = 0.1$, $\omega = 0.5$, $g = 0.5$, $\zeta_{ir} = 0.01$ and $P^* = 1000$.

exp(−0.4) of radiative energy emitted towards the nonirradiated face by the hot irradiated face was absorbed by the nonirradiated face. The first peak was observed at the end of irradiation pulse. After irradiation turn-off, due to the radiation cooling of surrounding, first, the temperature of the nonirradiated face decreases gradually, and then the temperature of the nonirradiated face increases due to the heat conducted from the hot face, and the second peak will be observed.

Recently, laser flash method was often used to measure the thermal conductivity or diffusivity of solid material [26]. For opaque solid, thermal diffusivity can be easily determined from the temperature evolution curve of nonirradiated surface, and the related formula is very simple. For semitransparent solid, the temperature evolution curves differ significantly from that of opaque solid. For the sake of comparison, we calculated the temperature responses of two cases, one takes into account the radiation in medium, the other does not. The input parameters are taken as $N = 7$, $n = 1$, $\tau_L = 0.4$, $\tau_R = 0.1$, $\omega = 0.5$, $g = 0.5$, $\zeta_{ir} = 0.01$ and $P^* = 1000$. The results are shown in *figure 5*. We can see that the difference of temperature evolution curves between the two cases is larger. For semitransparent medium, even in the conduction-dominated case, the application of laser flash method in thermal metrology may give irrelevant results if the radiation is not taken into account.

Figure 6 shows the effects of refractive index n on the transient temperature responses. The effect of refractive index on the temperature responses is significant. *Figure 7* shows the effects of axial optical thickness τ_L on the transient temperature responses. The effect of axial optical thickness on the temperature evolution curves of nonirradiated end surface is greater than that of irradiated end surface, and the temperature peak value of the nonirradiated end surface decreases obviously with the increase of axial optical thickness.

Figure 8 shows the effect of dimensionless amplitude of pulse irradiation P^* on the transient temperature responses. The temperature responses increase obviously with the increase of the dimensionless amplitude of pulse irradiation. *Figure 9* shows the effect of the dimensionless time width of pulse irradiation ζ_{ir}. The temperature responses are evidently affected by the dimensionless time width of pulse irradiation. With the increase of ζ_{ir}, the peak temperature increases, and the temperature responses last longer.

Figure 10 shows the influences of the single scattering albedo ω on the temperature responses. As shown in *figure 10(a)*, the effects of the single scattering albedo ω on the irradiated surface of $\tau_z = 0$ are very small,

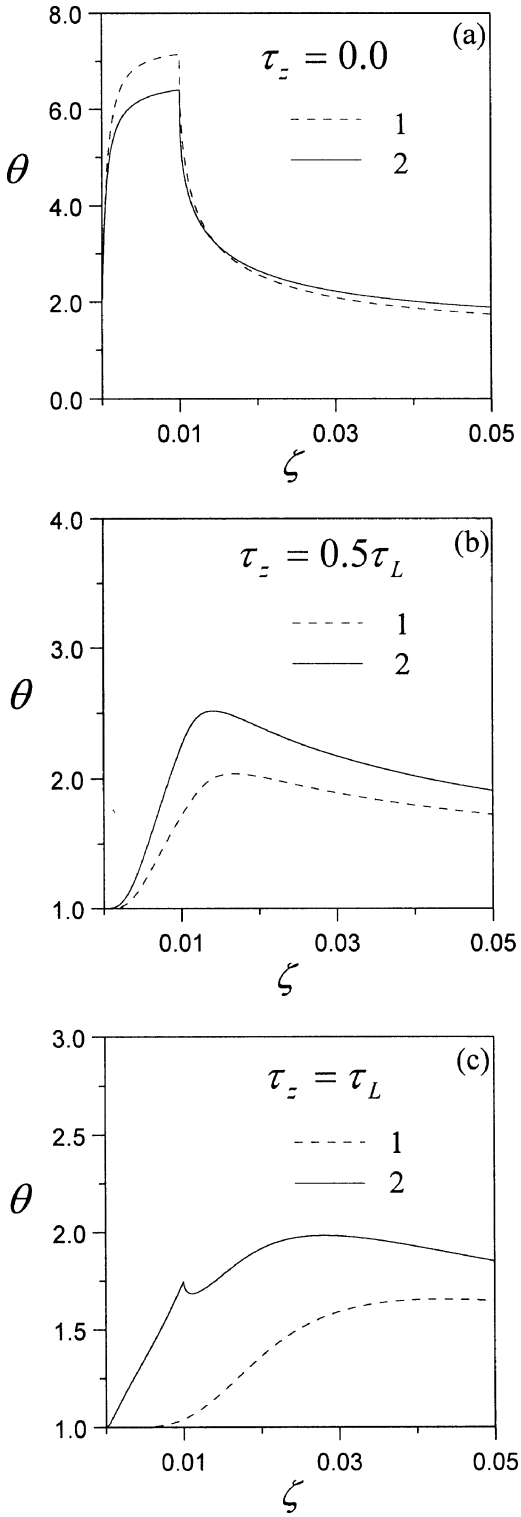

Figure 5. The calculated temperature responses for the following two cases, one takes into account the radiation in medium (curve 2), the other does not (curve 1).

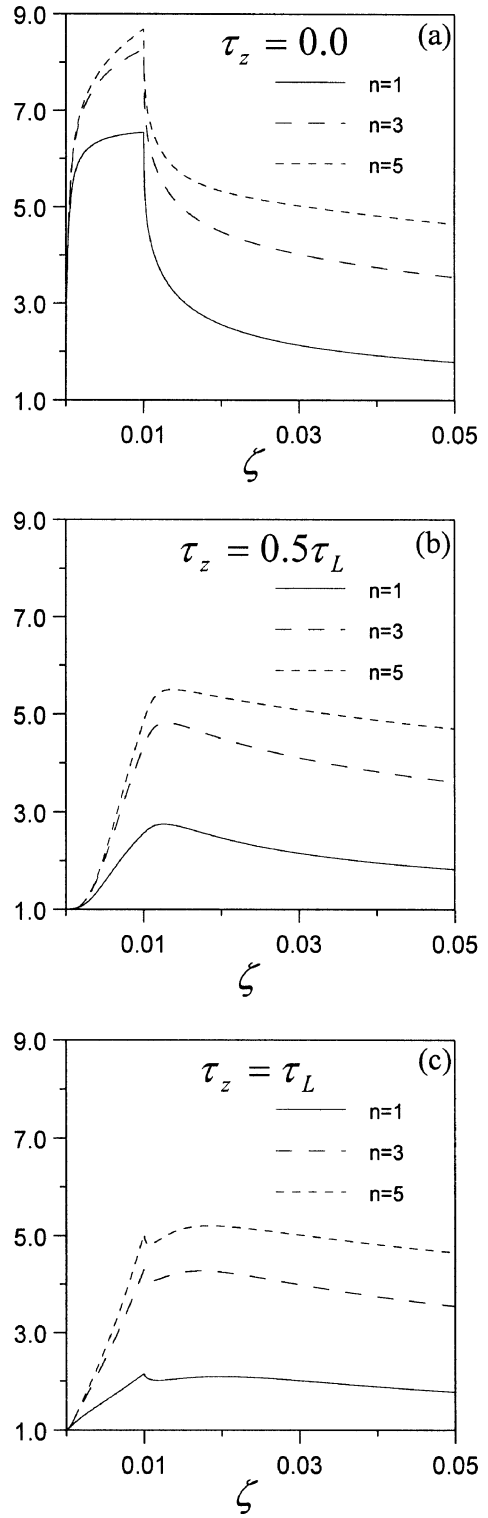

Figure 6. The effect of the refractive index n on the transient temperature responses in the case of $N = 5$, $\tau_L = 0.4$, $\tau_R = 0.1$, $\omega = 0.5$, $g = 0.5$, $\zeta_{ir} = 0.01$ and $P^* = 1000$.

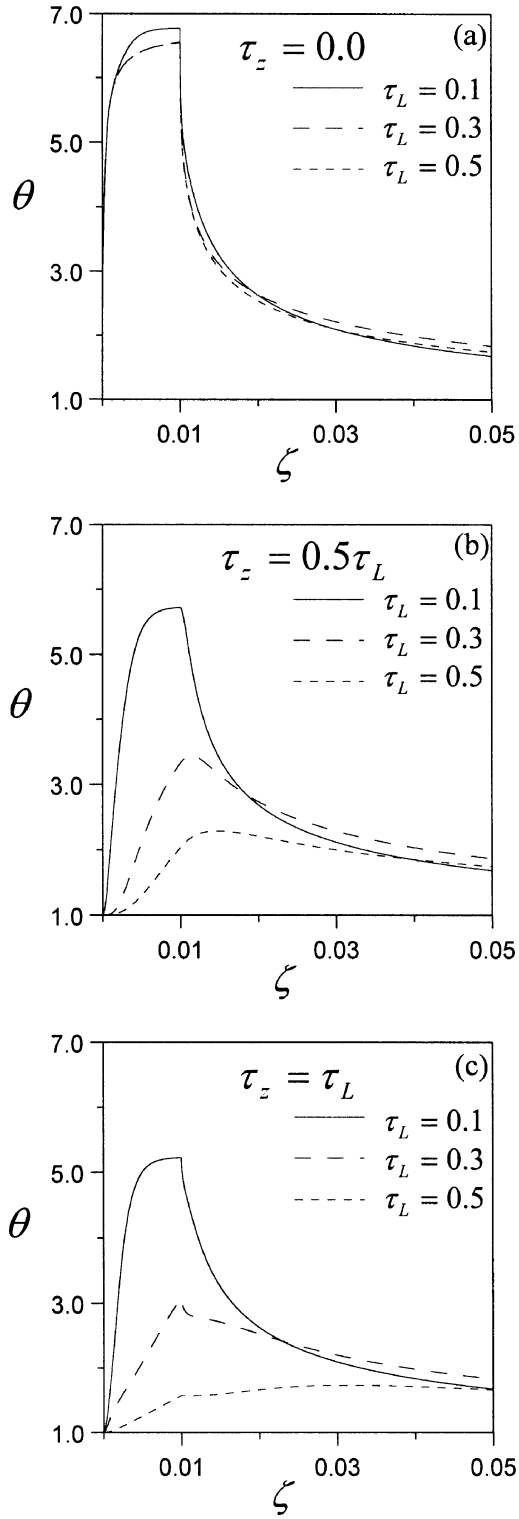

Figure 7. The effect of the axial optical thickness τ_L on the transient temperature responses in the case of $N = 5$, $n = 1$, $\tau_R = 0.1$, $\omega = 0.5$, $g = 0.5$, $\zeta_{ir} = 0.01$ and $P^* = 1000$.

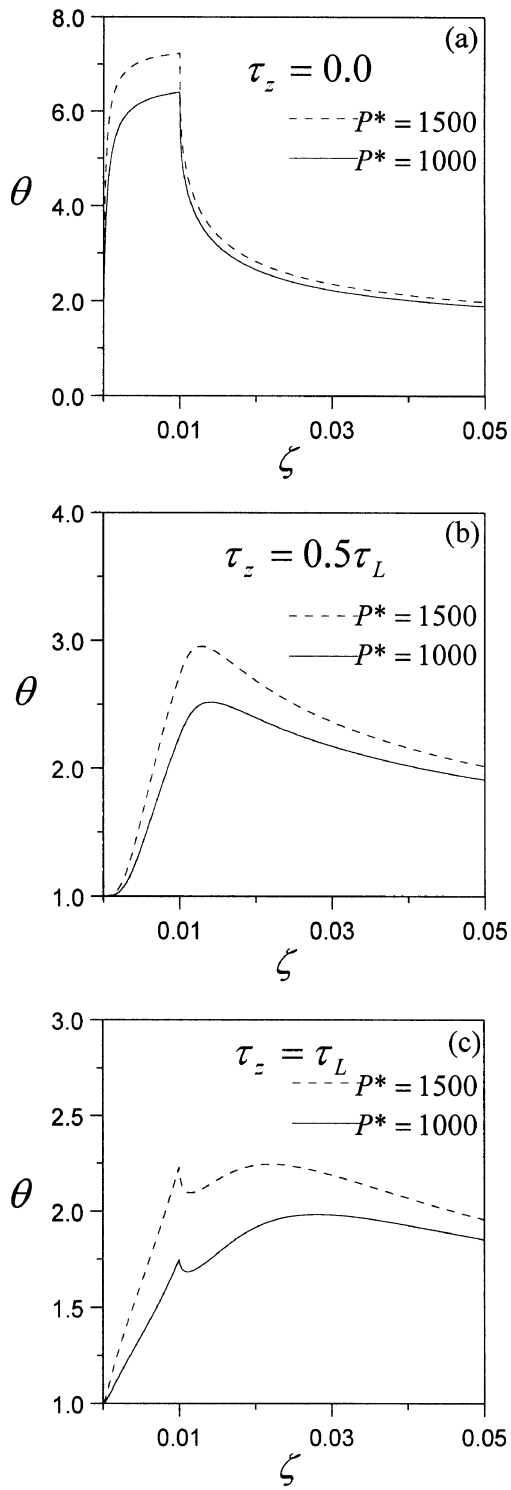

Figure 8. The effect of the dimensionless amplitude of pulse irradiation P^* on the transient temperature responses in the case of $N = 7$, $n = 1$, $\tau_L = 0.4$, $\tau_R = 0.1$, $\omega = 0.5$, $g = 0.5$ and $\zeta_{ir} = 0.01$.

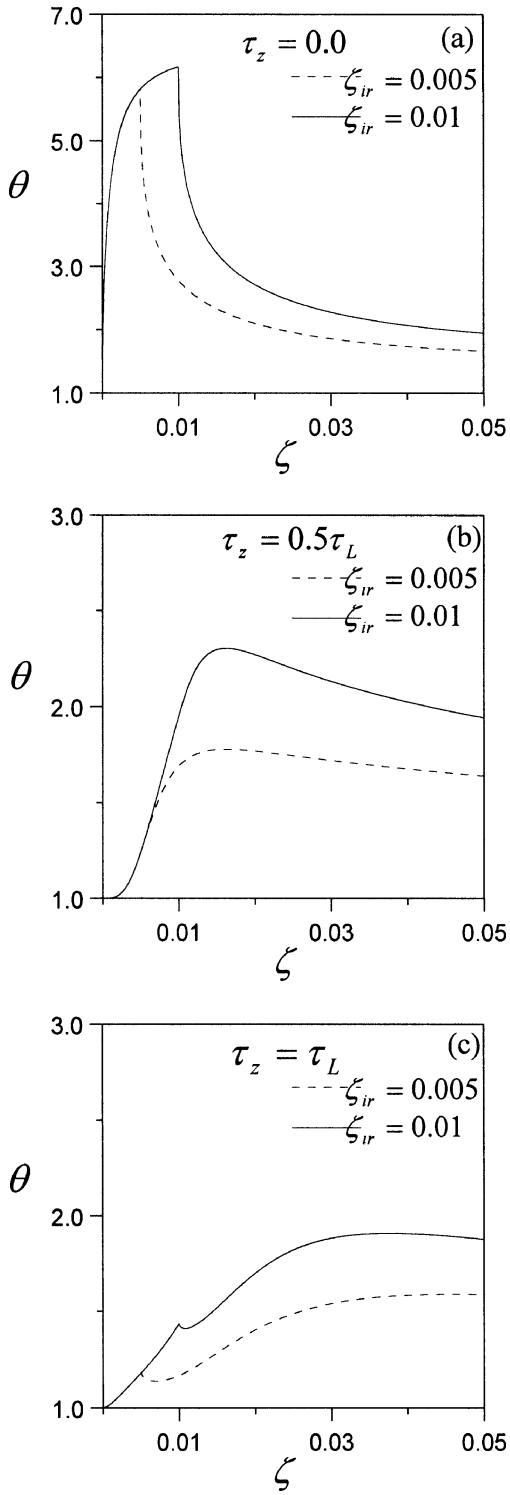

Figure 9. The effect of the dimensionless time width of pulse irradiation ζ_{ir} on the transient temperature responses in the case of $N = 10$, $n = 1$, $\tau_L = 0.4$, $\tau_R = 0.1$, $\omega = 0.5$, $g = 0.5$ and $P^* = 1000$.

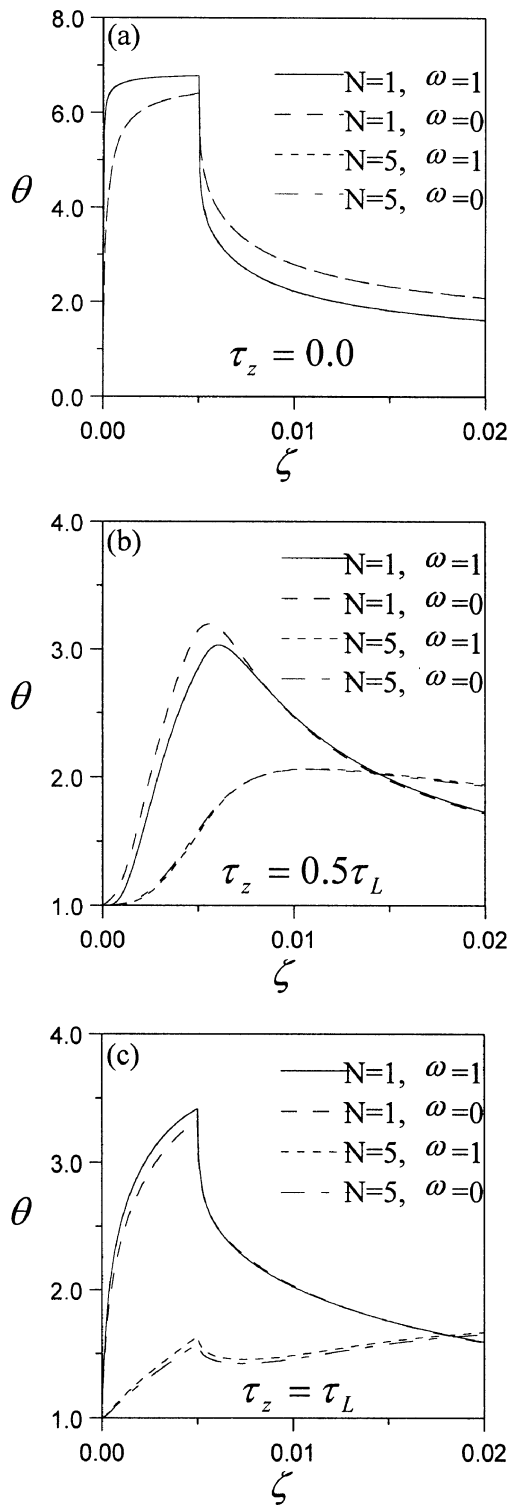

Figure 10. The influences of the single scattering albedo ω on the temperature responses in the case of $n = 1$, $\tau_L = 0.4$, $\tau_R = 0.1$, $g = 0.5$, $\zeta_{ir} = 0.005$ and $P^* = 1000$.

and no observable difference could be detected between the results of $\omega = 1.0$ and $\omega = 0.0$ when the results are presented in graphical form. The effects of single-scattering albedo on the midplane ($\tau_z = 0.5\tau_L$) and the nonrridiated end surface ($\tau_z = \tau_L$) are shown in *figures 10 (b)* and *(c)*, respectively. For the conduction-dominated case ($N = 5$), the variation of temperature evolution curves for different single-scattering albedo is very small. With the decrease of conduction-to-radiation parameter N, the effects of single-scattering albedo increase significantly.

5. CONCLUSIONS

The transient thermal responses in a two-dimensional semitransparent cylinder with black boundary surface caused by a pulse irradiation at one end of the cylinder are studied. The processes of the transient coupled radiative–conductive heat transfer in the cylinder are analyzed numerically. An implicit central-difference scheme is employed for handling the energy equation, while a discrete-ordinates method is used to solve the radiative transfer equation. The effects of various parameters on the transient thermal responses are investigated. The main conclusions can be summarized as follows:

(1) Due to the radiation within medium, the transient temperature of the nonirradiated end surface ($\tau_z = \tau_L$) of the cylinder can be greater than that of the inner medium of cylinder. Under some conditions, the temperature evolution curves with two peaks can be observed in the nonirradiated end of the cylinder. For semitransparent medium, even in the conduction-dominated case, application of laser flash method in thermal metrology may give irrelevant results if the radiation is not taken into account.

(2) The temperature responses increase obviously with the increase of the dimensionless amplitude of pulse irradiation. The temperature responses are obviously affected by the dimensionless time width of pulse irradiation. With the increase of ζ_{ir}, the peak temperature increases, and the temperature responses last longer.

(3) The effects of the conduction-radiation parameter, the optical thickness and the refractive index are large. The effects of the single-scattering albedo are more significant for the radiation-dominated case than that for the conduction-dominated case.

Acknowledgements

The supports of this work by the Fok Ying Tung Education Foundation, the Chinese National Science Fund for Distinguished Young Scholar and the Scientific Research Foundation of Harbin Institute of Technology are gratefully acknowledged.

REFERENCES

[1] Viskanta R., Heat transfer by conduction and radiation in absorbing and scattering materials, ASME J. Heat Transfer 87 (1965) 143–150.

[2] Lii C.C., Ozisik M.N., Transfer radiation and conduction in an absorbing, emitting, scattering slab with refecting boundaries, Internat. J. Heat Mass Transfer 15 (1972) 1175–1179.

[3] Amlin D.W., Korpela S.A., Influence of thermal radiation on the temperature distribution in a semitransparent solid, ASME J. Heat Transfer 101 (1979) 76–80.

[4] Siewert C.E., Thomas J.R. Jr, A computational method for solving a class of coupled conductive radiative heat transfer problems, J. Quant Spectrosc Radiant Transfer 45 (1991) 273–281.

[5] Siewert C.E., Thomas J.R. Jr, On coupled conductive radiative heat transfer problems in a sphere, J. Quant Spectrosc Radiant Transfer 46 (1991) 63–72.

[6] Siewert C.E., Thomas J.R. Jr, On coupled conductive radiative heat transfer problems in a cylinder, J. Quant Spectrosc Radiant Transfer 48 (1992) 227–236.

[7] Siewert C.E., An improved iterative method for solving a class of coupled conductive radiative heat transfer problems, J. Quant Spectrosc Radiant Transfer 54 (1995) 599–605.

[8] Derevyanko G.V., Koltun P.S., Radiative–conductive heat transfer of semitransparent bodies, J. Engrg. Phys. Thermophys. 61 (1992) 1302–1305.

[9] Vargas R., de Vilhena M.T., A closed form solution for the one-dimensional radiative conductive problem by the decomposition and LTS_N methods, J. Quant Spectrosc Radiant Transfer 61 (1999) 303–308.

[10] Abulwafa E.M., Conductive radiative heat transfer in an inhomogeneous plane-parallel medium using Galerkin-iterative method, J. Quant Spectrosc Radiant Transfer 61 (1999) 583–589.

[11] Tan H.P., Maestre B., Lallemand M., Transient and steady-state combined heat transfer in semitransparent materials subjected to a pulse or a step irradiation, ASME J. Heat Transfer 113 (1991) 166–173.

[12] Tan H.P., Ruan L.M., Tong T.W., Temperature response in absorbing, isotropic scattering medium caused by laser pulse, Internat. J. Heat Mass Transfer 43 (2000) 311–320.

[13] Andre S., Degiovanni A., A theoretical study of the transient couple conduction and radiation heat transfer in glass: phonic diffusivity measurements by flash technique, Internat. J. Heat Mass Transfer 38 (1995) 3401–3414.

[14] Hahn O., Raether F., Arduini-Schuster M.C., Fricke J., Transient coupled conductive/radiative heat transfer in absorbing, emitting and scattering media: application to laser-flash measurements on ceramic materials, Internat. J. Heat Mass Transfer 40 (1997) 689–698.

[15] Mehling H., Hautzinger G., Nilsson O., Fricke J., Hofmann R., Hahn O., Thermal diffusivity of semitransparent materials determined by the laser-flash method apply-

ing a new analytical model, Internat. J. Thermophysics 19 (1998) 941–949.

[16] Spuckler C.M., Siegel R., Refractive index effects on radiative behavior of a heated absorbing-emitting layer, J. Thermophys Heat Transfer 6 (1992) 596–604.

[17] Spuckler C.M., Siegel R., Refractive index and scattering effects on radiative behavior of a semitransparent layer, J. Thermophys Heat Transfer 7 (1993) 302–310.

[18] Sakami M., Charette A., Le Dez V., Application of the discrete ordinates method to combined conductive and radiative heat transfer in a two-dimensional complex geometry, J. Quant. Spectrosc. Radiative Transfer 56 (1996) 517–533.

[19] Li H.Y., Ozisik M.N., Simultaneous conduction and radiation in a two-dimensional participating cylinder with anisotropic scattering, J. Quant. Spectrosc. Radiative Transfer 46 (1991) 393–404.

[20] Le Dez V., Vaillon R., Lemonier D., Lallemand M., Conductive–radiative coupling in an absorbing-emitting axisymmetric medium, J. Quant. Spectrosc. Radiative Transfer 65 (2000) 787–803.

[21] Wu K.H., Wu C.Y., Transient two-dimensional radiative and conductive heat transfer in an axisymmetric medium, Heat and Mass Transfer 33 (1998) 327–331.

[22] Jones P.D., Bayazitoglu Y., Coordinate system for the radiative transfer equation in curvilinear media, J. Quant. Spectrosc. Radiative Transfer 48 (1992) 427–440.

[23] Patankar S.V., Numerical Heat Transfer and Fluid Flow, Hemisphere, New York, 1980.

[24] Liu L.H., Yu Q.Z., Tan H.P., Ruan L.M., Discrete ordinate solutions of radiative transfer equation, Chinese J. Comput. Phys. 15 (1998) 337–343.

[25] Modest M.F., Radiative Heat Transfer, McGraw-Hill, New York, 1993.

[26] Stephen D.P., A review of techniques for measuring the thermal diffusivity of thin films and coatings, High Temperature—High Pressures 27 (1996) 111–134.